Am J Physiol Heart Circ Physiol 289: H1798–H1806, 2005.
First published July 8, 2005; doi:10.1152/ajpheart.01309.2004.

TRANSLATIONAL PHYSIOLOGY

Myocardial perfusion reserve in adults with cyanotic congenital heart disease

Richard C. Brunken,[1] Joseph K. Perloff,[2] Johannes Czernin,[1] Roxana Campisi,[1] Susan Purcell,[1] Pamela D. Miner,[2] John S. Child,[2] and Heinrich R. Schelbert[1]

[1]*Department of Molecular and Medical Pharmacology and the* [2]*Ahmanson/University of California, Los Angeles, Adult Congenital Heart Disease Center, David Geffen School of Medicine at The University of California, Los Angeles, California*

Submitted 1 January 2004; accepted in final form 16 June 2005

Brunken, Richard C., Joseph K. Perloff, Johannes Czernin, Roxana Campisi, Susan Purcell, Pamela D. Miner, John S. Child, and Heinrich R. Schelbert. Myocardial perfusion reserve in adults with cyanotic congenital heart disease. *Am J Physiol Heart Circ Physiol* 289: H1798–H1806, 2005. First published July 8, 2005; doi:10.1152/ajpheart.01309.2004.—In patients with cyanotic congenital heart disease (CCHD), a right-to-left shunt results in systemic hypoxemia. Systemic hypoxemia incites a compensatory erythrocytosis, which increases whole blood viscosity. We considered that these changes might adversely influence myocardial perfusion in CCHD patients. Basal and hyperemic (intravenous dipyridamole) perfusion measurements were obtained with [^{13}N]ammonia positron emission tomographic imaging in left (LV) and right (RV) ventricular and septal myocardium in 14 adults with CCHD [age: 34.1 yr (SD 6.5)]; hematocrit: 62.2% (SD 4.8)] and 10 healthy controls [age: 34.1 yr (SD 6.5)]. In patients, basal perfusion measurements were higher in LV [0.77 (SD 0.24) vs. 0.55 ml·min^{-1}·g^{-1} (SD 0.09), $P < 0.02$], septum [0.71 (SD 0.16) vs. 0.49 ml·min^{-1}·g^{-1} (SD 0.09), $P < 0.001$], and RV [0.77 (SD 0.30) vs. 0.38 ml·min^{-1}·g^{-1} (SD 0.09), $P < 0.001$]. However, basal measurements normalized for the rate-pressure product were similar to those of controls. Calculated oxygen delivery relative to rate-pressure product was higher in the patients [2.2 (SD 0.8) vs. 1.6 (SD 0.4) $\times$ 10^{-5} ml O_2·min^{-1}·g tissue^{-1}·(beats·mmHg)$^{-1}$ in the LV, $P < 0.05$, and 2.0 (SD 0.7) vs. 1.4 (SD 0.3) $\times$ 10^{-5} ml O_2·min^{-1}·g tissue^{-1}·(beats·mmHg)$^{-1}$ in the septum, $P < 0.01$]. Hyperemic perfusion measurements in CCHD patients did not differ from controls [LV, 1.67 (SD 0.60) vs. 1.95 ml·min^{-1}·g^{-1} (SD 0.46); septum, 1.44 (SD 0.56) vs. 1.98 ml·min^{-1}·g^{-1} (SD 0.69); RV, 1.56 (SD 0.56) vs. 1.65 ml·min^{-1}·g^{-1} (SD 0.64), P = not significant], and coronary vascular resistances were comparable [LV, 55 (SD 25) vs. 48 mmHg·ml^{-1}·g·min (SD 16); septum, 67 (SD 35) vs. 50 mmHg·ml^{-1}·g·min (SD 21); RV, 59 (SD 26) vs. 61 mmHg·ml^{-1}·g·min (SD 27), P = not significant]. These findings suggest that adult CCHD patients have remodeling of the coronary circulation to compensate for the rheologic changes attending chronic hypoxemia.

heart defects congenital; myocardial perfusion; positron emission tomography; myocardial perfusion reserve

IN PATIENTS with cyanotic congenital heart disease (CCHD), infusion of poorly oxygenated blood into the systemic circulation via a right-to-left shunt results in sustained arterial hypoxemia. Arterial hypoxemia accelerates the release of erythropoetin from specialized sensor cells in the renal cortex, which in turn increases the number of circulating red blood cells (erythrocytosis) and the arterial hemoglobin concentration (17, 25). This adaptive response helps to sustain tissue oxygen delivery, with equilibrium conditions typically being reached at elevated hematocrit levels (42). Oxygen delivery might also be augmented in the peripheral tissues of CCHD patients by an increase in oxygen extraction (3). However, this mechanism appears to be of limited utility for the coronary microcirculation, because resting oxygen extraction in the healthy human myocardium is already high and approaches 70% under basal conditions (23). This suggests that increases in myocardial oxygen demand need to be accompanied by nearly parallel increases in perfusion to sustain aerobic metabolism. Measurements of myocardial perfusion have previously been made in a small number of CCHD patients during cardiac catheterization, using clearance rates of inert gases or iodine-131 iodoantipyrine (51, 53). These early studies were limited by the methodology used to measure the tracer clearance rates and were further confounded by the need to normalize blood flows to derived estimates of ventricular mass. Moreover, these studies provided information only about global, and not regional, myocardial perfusion.

Erythrocytosis increases whole blood viscosity in a nonlinear fashion (30, 46). In vivo measurements made with intravital microscopy, for example, indicate that a change in hematocrit from 45% to 65% increases whole blood viscosity by about 60% and nearly doubles microvascular resistance (46). Because prior clinical reports suggest that marked increases in red blood cell mass might impair myocardial perfusion (27, 61), it has been proposed that the erythrocytosis in CCHD may be more detrimental than beneficial for some patients. On the other hand, more recent studies indicate that increases in perfusate viscosity are associated with increases in shear stress, which could serve to stimulate circulatory remodeling via several mechanisms, including augmented expression of vascular endothial growth factor and upregulated production of nitric oxide (7, 14, 20, 29, 35, 47, 50, 56, 57). Circulatory remodeling might benefit myocardial perfusion by increasing the size of existing vessels and stimulating new vessel growth. Prior clinical reports and recent angiographic studies do indicate that the extramural coronary arteries may be dilated in CCHD patients (5, 11, 41). However, little is known regarding regional tissue perfusion in CCHD patients, either in the basal state or during stress. Accordingly, the goal of this investigation was to compare basal and hyperemic regional myocardial perfusion measurements made noninvasively with positron emission tomography (PET) in adult CCHD patients to those in control subjects.

Address for reprint requests and other correspondence: R. C. Brunken, Dept. of Molecular and Functional Imaging/Gb3, Cleveland Clinic Foundation, 9500 Euclid Ave., Cleveland, OH 44195 (e-mail: brunker@ccf.org).

The costs of publication of this article were defrayed in part by the payment of page charges. The article must therefore be hereby marked "*advertisement*" in accordance with 18 U.S.C. Section 1734 solely to indicate this fact.

MATERIALS AND METHODS

Study population. Fourteen consecutive patients [7 male, age 34.1 yr (SD 6.5)] with echocardiographically confirmed CCHD were prospectively studied (10). Thirteen had Eisenmenger's syndrome and one had double-outlet right ventricle with pulmonic stenosis. On echocardiography, end-diastolic and end-systolic wall thicknesses averaged 12 (SD 4) and 15 mm (SD 6) in the septum, 10 (SD 2) and 13 mm (SD 3) in the left ventricular (LV) free wall, and 12 (SD 3) and 15 mm (SD 5) in the right ventricular (RV) free wall. Hematocrits averaged 62.2% (SD 4.8) (range: 54.8–70.8%). Mean hemoglobin was 20.7 g/dl (SD 1.9) (range: 17.8–23.9 g/dl). All were studied in an iron-replete state, because deficiency results in microspherocytes that increase blood viscosity (22, 34).

Ten healthy volunteers (9 male), with a comparable male-to-female ratio ($P = 0.08$, Fisher's exact test) and age [37.8 yr (SD 4.8)], were controls. None had diabetes or hypertension or used tobacco products or sympathomimetic drugs. Each refrained from caffeine or theobromine-containing foods for 24 h before imaging. Each of the CCHD patients and controls signed an informed consent form approved by the University of California, Los Angeles Medical Center Institutional Review Board.

PET. Baseline and dipyridamole stress dynamic [^{13}N]ammonia perfusion images were obtained using a CTI-Siemens 931/8 tomograph according to previously reported methods (12). After the patient was positioned in the scanner and a 20-min transmission scan was acquired, basal perfusion images were obtained after the intravenous administration of 15–20 mCi of [^{13}N]ammonia. After the physical decay of ^{13}N, 0.56 mg/kg of dipyridamole was infused intravenously over a 4-min time interval. Stress perfusion images were then recorded following the administration of a second dose of [^{13}N]ammonia 4 min after the end of the dipyridamole infusion. Serial basal and stress perfusion images were each acquired for 19 min (12 frames of 10 s each, two frames of 30 s, one frame of 60 s, and one frame of 900 s). Cuff blood pressures and 12 lead electrocardiograms were obtained each minute during stress. Peripheral arterial oxygen saturation was continuously monitored using a pulse oximeter.

The serially acquired [^{13}N]ammonia transaxial image sets were reoriented into short-axis images on a MacIntosh computer workstation using the CALIPSO software package for medical image processing employing previously reported methods (44). Large regions of interest (ROIs), encompassing about two-thirds of the visualized structure, were assigned on the last frames of the reoriented [^{13}N]ammonia short-axis perfusion images to the LV free wall, RV free wall, and septum. Septal regions were drawn to exclude the superior and inferior insertions of the RV myocardium. Regions were assigned on the short-axis images at apical, midventricular, and basal levels. Two 25-mm^2 ROI were assigned on the most basal short-axis images to the RV and LV blood pools. The scanner's spatial resolution did not permit separate definition of RV septal and LV septal myocardium. Decay-corrected time-activity curves from the ROIs were corrected for partial volume using recovery coefficients based on measured echocardiographic wall thicknesses in patients and by the use of normal values according to body surface area in controls (55). Time-averaged wall thicknesses were obtained by dividing the sum of the end-systolic and twice the end-diastolic dimensions by three. Recovery coefficients for each thickness were defined by the established performance characteristics of the tomograph (16).

Septal and LV perfusion measurements were obtained by fitting time activity curves with a two-compartment tracer kinetic model that corrects for blood pool spillover (31, 32). RV values were calculated by using a modified model, in which spillover is estimated by using a RV blood pool time-activity curve (8). Perfusion measurements from the apical, midventricular, and basal short-axis slices were averaged for LV, RV, and septum to yield a mean value for each myocardial region for each patient. Hyperemic values were divided by basal measurements to calculate perfusion reserves. In animal studies, the accuracy of the PET measurements has been determined relative to measurements obtained with simultaneously administered radioactive microspheres (4, 6, 8, 32, 38). The 95% confidence limits are about ± 0.33 ml·min^{-1}·g^{-1} for the LV measurements and ± 0.57 ml·min^{-1}·g^{-1} for the RV measurements. In human studies, interobserver variability is about 0.04 ml·min^{-1}·g^{-1} for the basal perfusion measurements, 0.17 ml·min^{-1}·g^{-1} for the stress measurements, and 0.36 for the perfusion reserve determinations (13, 39, 52).

Mean aortic pressures were divided by perfusion values to derive estimates of coronary vascular resistances (15). The oxygen content of the blood was calculated using the equation: O_2 content (in ml O_2/ml of blood) = 1.34 (ml oxygen/g of hemoglobin) × hemoglobin concentration (in g/ml) × the percent arterial oxygen saturation. Oxygen content in the normal volunteers was calculated using the corresponding mean laboratory hemoglobin concentration for males (14.3 g/dl) and females (13.1 g/dl) and the mean normal laboratory arterial oxygen saturation of 98%. Oxygen delivery to the myocardium (in ml O_2·min^{-1}·g tissue^{-1}) was calculated by multiplying the oxygen content of the blood by the PET perfusion measurements (expressed as ml blood·min^{-1}·g tissue^{-1}).

Statistical analysis. Means (SD) are reported. Probabilities <0.05 were considered significant. Data were analyzed using Systat (Systat Software, Richmond CA). Individual paired data were analyzed with the paired *t*-test. Patients' and volunteers' hemodynamic variables were compared using the unpaired *t*-test. Basal and hyperemic perfusion measurements and perfusion reserves were compared by region and between groups using analysis of variance, employing the Tukey test to identify intergroup differences. Stepwise linear regression analysis was used to relate the clinical variables and baseline perfusion values to hyperemic measurements, with an alpha level of 0.15. Multivariate linear regression analysis was then utilized to identify the parameters related to the hyperemic perfusion measurements.

RESULTS

Heart rate, blood pressure, and double product. Measurements of heart rate, systolic blood pressure, and rate-pressure product (RPP) were utilized to assess ventricular workloads and thus provide an indirect index of myocardial oxygen demand. Basal heart rates were higher in the patients than in the controls (Table 1) but similar during stress. Basal systolic

Table 1. *Hemodynamics during cardiac PET imaging*

	Patients	Controls	Probability
n	14	10	
HR, beats/min			
Rest	77.6 (10.9)	57.9 (10.3)	<0.0002
Stress	94.6 (16.5)	86.4 (12.5)	NS
Δ HR	17.0 (14.3)	28.5 (4.2)	<0.05
Systolic BP, mmHg			
Rest	107.6 (11.2)	114.2 (10.8)	NS
Stress	106.6 (13.6)	121.7 (16.0)	<0.05
Δ Systolic BP	−1.0 (7.1)	7.5 (9.7)	<0.05
Diastolic BP, mmHg			
Rest	70.6 (11.1)	70.7 (8.7)	NS
Stress	65.7 (10.0)	69.7 (12.1)	NS
Δ Diastolic BP	−4.9 (3.7)	−1.0 (11.5)	NS
MAP, mmHg			
Rest	82.9 (10.9)	85.2 (9.1)	NS
Stress	79.2 (10.8)	87.0 (12.5)	NS
Δ MAP	−3.7 (3.9)	1.8 (10.3)	NS
RPP			
Rest	8,408 (1,885)	6,615 (1,347)	<0.02
Stress	10,181 (2,705)	10,576 (2,501)	NS
Δ RPP	1,772 (1,931)	3,961 (1,447)	<0.01

Values are means (SD); *n*, number of subjects. PET, positron emission tomography; HR, heart rate; BP, blood pressure; MAP, mean arterial pressure; RPP, rate-pressure product; NS, not significant. Δ Parameter change from rest to stress.

blood pressures were comparable in both groups. During pharmacological stress, patients exhibited no change in systolic blood pressure, whereas it increased modestly in controls ($P < 0.05$). Mean basal and hyperemic arterial blood pressures were similar in each group. The patients' RPP were higher at baseline, implying greater ventricular workloads in the basal state. RPP values during stress were virtually identical to the controls, suggesting comparable ventricular workloads. Mean arterial oxygen saturation in the CCHD patients during stress was 86.2% (SD 2.1) and did not differ from that at baseline [83.9% (SD 2.6)].

Basal perfusion measurements and myocardial O_2 delivery. Measurements were made in 30 LV, 30 septal, and 24 RV ROIs in controls and in 33 LV, 27 septal, and 33 RV ROIs in patients (Tables 2 and 3). Septal values were not obtainable in one patient with a large ventricular septal defect. Measurements from the apical, midventricular, and basal short-axis ROIs were averaged to give a mean value for LV, RV, and septum in every subject. Control LV and septal values averaged 0.55 (SD 0.09) and 0.49 $ml \cdot min^{-1} \cdot g^{-1}$ (SD 0.09) (P = not significant, Fig. 1). RV values averaged 0.38 $ml \cdot min^{-1} \cdot g^{-1}$ (SD 0.09), which were lower than in LV ($P < 0.001$) or

Table 2. *Hemodynamic and perfusion data in congenital heart disease patients*

Pt	Age, yr	Clinical Diagnosis	Hct, %	Hb		HR, beats/min	Systolic BP, mmHg	Mean BP, mmHg	Myocardial Perfusion, $ml \cdot min^{-1} \cdot g^{-1}$ RV	septum	LV
1	35	VSD	70.8	23.9	Basal	83	102	85	0.61	0.55	0.47
					Stress	115	104	84	1.00	0.74	0.86
					WT				15	23	11
2	39	Truncus art.	54.8	18.8	Basal	77	110	83	0.88	0.55	0.63
					Stress	93	99	78	1.89	1.79	1.82
					WT				20	22	14
3	32	ASD	69.7	23.6	Basal	100	112	89	0.43	0.39	0.61
					Stress	108	105	84	1.04	1.36	1.51
					WT				10	11	12
4	43	VSD	57.7	19.8	Basal	71	118	91	0.70	0.73	0.57
					Stress	116	124	88	2.27	2.37	2.57
					WT				15	15	14
5	35	ASD	64.1	21.6	Basal	99	138	111	0.73	0.64	0.88
					Stress	116	138	105	0.98	0.76	1.19
					WT				12	14	12
6	36	Dbl outlet RV/PS	61.4	21.2	Basal	78	106	79	1.51	Defect	1.20
					Stress	74	96	67	1.77	Defect	1.91
					WT				15	Defect	14
7	29	Truncus art.	67.0	23.1	Basal	83	91	67	1.27	0.80	0.95
					Stress	102	91	65	2.76	1.93	2.35
					WT				13	11	12
8	43	VSD	59.8	20.6	Basal	74	110	89	0.64	0.69	0.64
					Stress	79	116	88	1.06	0.87	1.12
					WT				12	11	11
9	30	TOGV/VSD; prior Mustard procedure	55.1	17.8	Basal	75	110	87	0.54	0.92	0.80
					Stress	97	105	80	1.89	1.80	2.69
					WT				16	13	10
10	20	TOGV/VSD	62.9	20.8	Basal	62	102	74	0.59	0.88	0.62
					Stress	95	94	67	1.74	1.81	1.29
					WT				11	10	9
11	30	Truncus art.	62.0	18.4	Basal	71	107	78	1.01	0.85	1.23
					Stress	99	122	82	1.18	1.71	1.95
					WT				10	11	9
12	38	VSD	59.9	19.3	Basal	67	103	77	0.52	0.78	0.78
					Stress	62	104	78	0.87	0.77	0.77
					WT				11	12	11
13	40	VSD	61.0	20.6	Basal	78	94	70	0.69	0.86	0.86
					Stress	88	93	68	1.62	1.89	1.79
					WT				9	11	9
14	27	TOGV/VSD; prior Mustard procedure	65.0	20.8	Basal	69	104	81	0.64	0.60	0.52
					Stress	81	102	76	1.82	0.92	1.63
					WT				5	8	7
		Mean (SD)			Basal	78 (11)	108 (11)	83 (11)	0.77 (0.30)	0.71 (0.16)	0.77 (0.24)
		Mean (SD)			Stress	95 (17)	107 (14)	79 (11)	1.56 (0.56)	1.44 (0.56)	1.67 (0.60)

Hct, hematocrit; Hb, hemoglobin; RV and LV, right and left ventricular myocardium, respectively; septum, interventricular septal myocardium; ASD and VSD, atrial and ventricular septal defects, respectively; Dbl Outl RV/PS, double outlet right ventricle with pulmonic stenosis; Truncus art., truncus arteriosus; TOGV, transposition of the great vessels; Mustard procedure, an operation in which an intraatrial pericardial baffle is created to redirect venous blood to the appropriate ventricle in patients with TOGV. WT, time averaged wall thickness (in mm), from echocardiographic measurements; basal and stress indicate measurements at baseline and during pharmacological stress.

Table 3. *Hemodynamic and perfusion data in the normal volunteers*

Subject	Age, yr		HR, beats/min	Systolic BP, mmHg	Mean BP, mmHg	Myocardial Perfusion, ml·min^{-1}·g^{-1}		
						RV	septum	LV
1	38	Basal	44	120	93	0.22	0.37	0.40
		Stress	77	128	93	1.50	2.44	2.26
		WT				4	11	12
2	43	Basal	52	105	79	0.88	0.42	0.60
		Stress	76	107	76	1.89	1.99	1.97
		WT				4	10	11
3	30	Basal	61	123	88	0.53	0.55	0.60
		Stress	91	141	90	0.88	1.13	2.01
		WT				4	10	11
4	38	Basal	55	120	93	0.32	0.41	0.61
		Stress	80	120	93	1.93	2.44	2.55
		WT				4	11	12
5	34	Basal	78	117	84	0.41	0.55	0.62
		Stress	112	146	113	1.19	1.28	1.42
		WT				4	11	12
6	40	Basal	72	115	89	0.51	0.63	0.52
		Stress	104	110	78	1.16	2.25	1.99
		WT				4	12	13
7	36	Basal	52	120	89	0.38	0.49	0.45
		Stress	83	129	93	2.74	2.03	1.81
		WT				4	13	14
8	35	Basal	60	98	70	0.36	0.56	0.48
		Stress	86	103	72	2.47	3.38	2.68
		WT				4	10	11
9	37	Basal	52	96	71	0.34	0.44	0.59
		Stress	80	101	73	1.70	1.59	1.57
		WT				4	10	11
10	47	Basal	53	128	95	0.32	0.37	0.67
		Stress	75	132	90	0.95	1.33	1.26
		WT				4	11	12
	Mean (SD)	Basal	58 (10)	114 (11)	85 (9)	0.38 (0.09)	0.49 (0.09)	0.55 (0.09)
	Mean (SD)	Stress	86 (13)	122 (16)	87 (13)	1.65 (0.64)	1.98 (0.69)	1.95 (0.46)

WT was estimated from echocardiographic measurements based on body surface area.

septum ($P < 0.05$). In the CCHD patients, basal perfusion measurements were comparable in each region and higher than those of controls (Fig. 1). Myocardial perfusion averaged 0.77 ml·min^{-1}·g^{-1} (SD 0.24) in LV ($P < 0.02$ vs. controls), 0.71 ml·min^{-1}·g^{-1} (SD 0.16) in septum ($P < 0.001$), and 0.77 ml·min^{-1}·g^{-1} (SD 0.30) in RV ($P < 0.001$).

CCHD patients had significantly higher basal myocardial oxygen delivery than the control subjects in all ventricular regions:

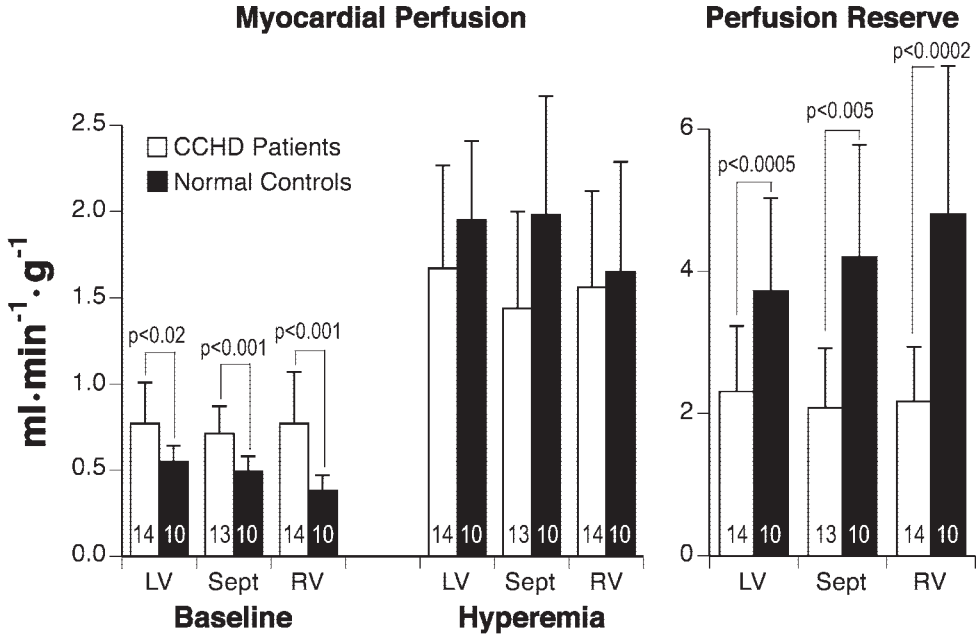

Fig. 1. Myocardial perfusion measurements in cyanotic congenital heart disease (CCHD) patients and age- and gender-matched control subjects. Patients had higher basal perfusion measurements than controls in each ventricular region. In CCHD patients, basal perfusion values were similar in each ventricular region. In controls, resting right ventricular (RV) perfusion measurements were lower than those in either the septum (Sept) or the left ventricle (LV). Regional hyperemic perfusion measurements were similar and did not differ between CCHD patients and controls. Within the patient group and within the control group, there were no differences in regional perfusion reserves. Perfusion reserves were greater in controls than in patients in each ventricular region.

0.18 (SD 0.06) vs. 0.10 ml $O_2 \cdot min^{-1} \cdot g$ tissue^{-1} (SD 0.02) for LV ($P < 0.0005$); 0.16 (SD 0.03) vs. 0.09 ml $O_2 \cdot min^{-1} \cdot g$ tissue^{-1} (SD 0.02) for septum ($P < 0.0001$); and 0.18 (SD 0.08) vs. 0.09 ml $O_2 \cdot min^{-1} \cdot g$ tissue^{-1} (SD 0.02) for RV ($P < 0.0005$).

Relationship to basal RPP. In previous studies, basal perfusion measurements have been shown to parallel myocardial oxygen consumption and to be linearly related to the RPP as an indirect index of this parameter (12, 36). To explore the impact of differences in basal RPP between the two groups on the perfusion measurements, septal and LV perfusion values were divided by the basal RPP values. When this was performed, LV and septal values in patients paralleled those of the control subjects: 9.47 (SD 3.39) vs. 8.59 (SD 1.86) $\times 10^{-5}$ $ml \cdot min^{-1} \cdot g^{-1} \cdot (beats \cdot mmHg)^{-1}$ for LV, $P = 0.79$; 8.95 (SD 3.05) vs. 7.61 (SD 1.60) $\times 10^{-5}$ $ml \cdot min^{-1} \cdot g^{-1} \cdot (beats \cdot mmHg)^{-1}$ for septum, $P = 0.22$.

However, when calculated myocardial oxygen delivery was normalized for ventricular work by dividing by the RPP, CCHD patients had significantly higher values than the controls in the LV [2.2 (SD 0.8) vs. 1.6 (SD 0.4) $\times 10^{-5}$ ml $O_2 \cdot min^{-1} \cdot g^{-1} \cdot (beats \cdot mmHg)^{-1}$] ($P < 0.05$, Fig. 2), and septum [2.0 (SD 0.7) vs. 1.4 (SD 0.3) $\times 10^{-5}$ ml $O_2 \cdot min^{-1} \cdot g^{-1} \cdot (beats \cdot mmHg)^{-1}$] ($P < 0.01$). This suggests that the higher tissue delivery of oxygen is not explicable solely on the basis of an increase in ventricular work. Because control RV pressure measurements were not available, and because of the inherent difficulties in estimating RV systolic pressures in patients with ventricular septal defects, a similar analysis for the RV measurements was not performed.

Hyperemic perfusion and flow reserve measurements. Hyperemic perfusion measurements were obtained in 30 LV, 30 septal, and 26 RV ROIs in controls and in 34 LV, 26 septal, and 33 RV ROIs in patients. Apical, midventricular, and basal hyperemic perfusion measurements were again averaged to give a mean value for LV, RV, and septum in every subject. During hyperemia, mean perfusion values increased significantly in both groups (Fig. 1 and Tables 2 and 3). Hyperemic values in controls were similar in each region, averaging 1.95 $ml \cdot min^{-1} \cdot g^{-1}$ (SD 0.46) in LV ($P < 0.0001$ vs. rest), 1.98 $ml \cdot min^{-1} \cdot g^{-1}$ (SD 0.69) in septum ($P < 0.00005$), and 1.65 $ml \cdot min^{-1} \cdot g^{-1}$ (SD 0.64) in RV ($P < 0.0005$). Perfusion reserves averaged 4.80 (SD 2.09) in RV, 3.72 (SD 1.31) in LV, and 4.20 (SD 1.58) in the septum ($P = 0.39$).

Hyperemic perfusion measurements in the CCHD patients were similar in each region and comparable to those in controls, averaging 1.67 $ml \cdot min^{-1} \cdot g^{-1}$ (SD 0.60) in LV ($P < 0.001$ vs. rest), 1.44 $ml \cdot min^{-1} \cdot g^{-1}$ (SD 0.56) in septum ($P < 0.002$), and 1.56 $ml \cdot min^{-1} \cdot g^{-1}$ (SD 0.56) in RV ($P < 0.001$). Perfusion reserves averaged 2.31 (SD 0.92) in LV, 2.08 (SD 0.84) in septum, and 2.17 (SD 0.77) in RV, significantly lower than in controls ($P < 0.005$ for LV, $P < 0.0005$ for septum and RV).

Coronary vascular resistances. In controls, estimates of basal RV resistances were higher than those for the LV, 239 (SD 82) vs. 158 $mmHg \cdot ml^{-1} \cdot g \cdot min$ (SD 35) ($P < 0.02$). Septal resistances averaged 180 $mmHg \cdot ml^{-1} \cdot g \cdot min$ (SD 48) and were comparable to RV ($P = 0.08$) and LV values ($P = 0.68$). In the CCHD patients, basal resistances were similar in each region. Resistances in LV and septum averaged 118 (SD 38) and 126 $mmHg \cdot ml^{-1} \cdot g \cdot min$ (SD 44) (each $P < 0.02$ vs. controls), whereas RV resistances averaged 122 $mmHg \cdot ml^{-1} \cdot g \cdot min$ (SD 43) ($P < 0.0002$).

Figure 3 illustrates the coronary vascular resistances during hyperemia. Dipyridamole reduced coronary resistances in controls ($P < 0.0002$ for RV, $P < 0.00002$ for LV and septum) and patients ($P < 0.0005$ for septum, $P < 0.00002$ for LV and RV). LV, septal and RV resistances in controls were similar at 48 (SD 16), 50 (SD 21), and 61 $mmHg \cdot ml^{-1} \cdot g \cdot min$ (SD 27), respectively. Regional resistances in patients were similar and comparable to those in controls, averaging 55 (SD 25), 67 (SD 35), and 59 $mmHg \cdot ml^{-1} \cdot g \cdot min$ (SD 26) in LV, septum, and RV.

Factors influencing hyperemic myocardial perfusion. Stepwise linear regression analysis was used to examine the relationship between hyperemic perfusion measurements (categorized by gender and myocardial region) and rest and stress heart rates; rest and stress systolic and diastolic blood pressures; rest and stress arterial oxygen saturations; and age, hemoglobin, hematocrit, and average wall thickness. A regression constant and terms for interactions between resting perfusion and heart rate, hematocrit and hemoglobin, and resting oxygen saturation and hematocrit were also used. This analysis

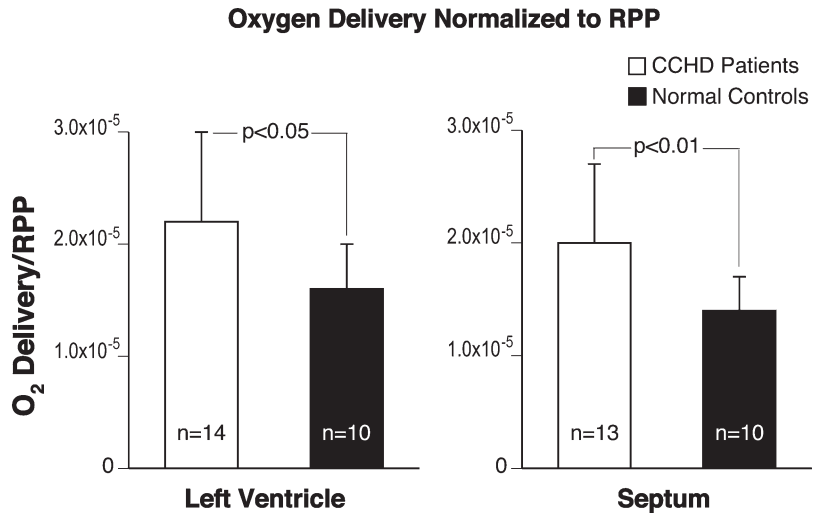

Fig. 2. Calculated oxygen delivery to myocardium in basal state, normalized to rate-pressure product (RPP) as an index of cardiac work [in ml $O_2 \cdot min^{-1} \cdot g$ tissue$^{-1} \cdot (beats \cdot mmHg)^{-1}$]. Oxygen delivery to LV and septum in CCHD patients is not compromised and exceeds that predicted by RPP as an index of cardiac work.

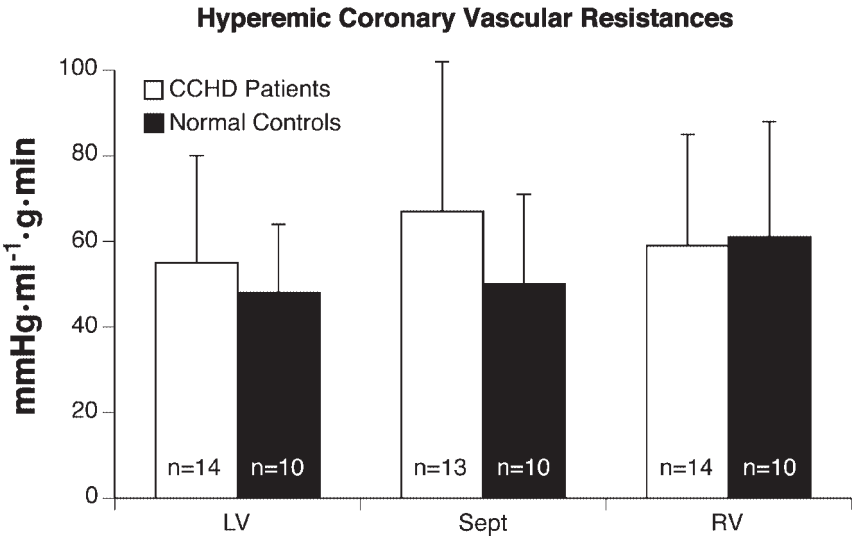

Fig. 3. Regional hyperemic coronary vascular resistances were similar in CCHD patients and controls.

identified the regression constant, resting perfusion, resting heart rate, stress systolic blood pressure, rest and stress arterial oxygen saturations, hematocrit and the term allowing for an interaction between resting arterial oxygen saturation and hematocrit as variables to test in a multivariate model. In the multivariate model, the regression constant, resting perfusion ($t = 2.7$, $P < 0.02$), resting heart rate ($t = 5.1$, $P < 0.0001$), stress systolic blood pressure ($t = 6.9$, $P < 0.00001$), and rest ($t = 2.1$, $P < 0.05$) and stress arterial oxygen saturations ($t = 3.7$, $P < 0.002$) were identified as variables influencing hyperemic blood flows.

DISCUSSION

To characterize myocardial perfusion in erythrocytotic adult patients with cyanotic congenital heart disease, basal and hyperemic perfusion measurements in RV, LV, and septum were obtained with PET in 14 adult CCHD patients and compared with those of age- and gender-matched control subjects. The study findings suggest that adult CCHD patients have a compensatory adaptation of their coronary circulation to the rheologic changes accompanying chronic systemic arterial hypoxemia.

Regional perfusion measurements. Basal myocardial perfusion in CCHD patients was similar in the RV, septum, and LV, suggesting comparable regional workloads and oxygen consumption. Because perfusion values were determined per gram of tissue, higher RV values in the patients relative to the controls cannot be explained by larger ventricular masses. Other factors, such as greater RV RPPs or coronary vascular remodeling, may explain these differences. Controls had basal RV values averaging about 69% of those in LV, consistent with a lower RV workload and comparable to values previously reported in awake nonhuman primates (28). Although septal measurements tended to be smaller than in LV, this did not achieve statistical significance.

Prior invasive measurements in CCHD. Rudolph (51) measured global myocardial perfusion during cardiac catheterization in 24 patients with Fallot's tetralogy, 24 patients with Eisenmenger's syndrome, and 7 "controls" with cor pulmonale. He also identified a relationship between resting myocardial perfusion and arterial oxygen saturation. Basal myocardial perfusion averaged 0.81 $ml \cdot min^{-1} \cdot g^{-1}$ in the patients with arterial oxygen saturations less than 80% and 0.75 $ml \cdot min^{-1} \cdot g^{-1}$ in those with saturations greater than 80%. These values appear smaller than his "control" values of 0.88 $ml \cdot min^{-1} \cdot g^{-1}$; however, statistical inferences about the differences are difficult to assess due to the manner in which the data are reported.

Scheuer and colleagues (53) determined myocardial perfusion at rest using iodine-131 iodoantipyrine clearance rates in seven CCHD patients during catheterization. Mean hematocrit of this population was 52.9% (SD 10.4), lower than that in our patients. Mean rest perfusion in his subjects averaged 0.72 $ml \cdot min^{-1} \cdot g^{-1}$ (SD 0.19), similar to our observations. In eight controls, rest myocardial perfusion averaged 1.02 $ml \cdot min^{-1} \cdot g^{-1}$ (SD 0.28). However, when Scheuer's perfusion measurements are normalized to the tension-time index as an index of oxygen consumption, our analysis of his data indicates that his patients and controls had comparable values.

Comparison of basal myocardial perfusion. Basal septal and LV values were higher in our patients than in controls. In part, this may reflect differences in ventricular work, because values were comparable when measurements were normalized for ventricular workload by dividing by the RPP. However, other factors might also influence myocardial perfusion. For example, vasodilators such as nitric oxide and prostaglandins released in response to the endothelial shear stress provoked by the erythrocytotic perfusate, as well as hypoxia-induced expression of vascular endothelium growth factor, might stimulate microcirculatory remodeling by angiogenesis and vasculogenesis and thereby augment basal perfusion (7, 14, 29, 35, 47, 50, 56, 57). In addition, structural alterations have been identified in the media of the epicardial coronary arteries and great vessels in CCHD patients (11, 40). It is conceivable that structural abnormalities might also exist in the smaller vessels in CCHD patients and contribute to vascular dilatation by weakening the vessel wall.

Hyperemic perfusion and perfusion reserves. Hyperemic septal and LV perfusion measurements in controls were slightly lower than values previously reported from our laboratory (12, 15). In those studies, correction for the partial volume effect was performed by using a fixed recovery coef-

ficient (assuming a 1.0-cm wall thickness). In the present study, time-averaged individualized recovery coefficients were used (to permit direct comparison to the CCHD patients with ventricular hypertrophy) and this may account for the observed differences.

Primarily due to lower basal measurements, RV perfusion reserves in controls tended to be higher than in other regions, but this did not achieve statistical significance. The mean RV perfusion reserve of 4.8 (SD 2.1) parallels the mean flow velocity reserve of 5.2 (SD 1.6) reported by Wilson and colleagues (60) for the right coronary artery in response to intravenous dipyridamole. Whereas intracoronary flow velocities differ from PET perfusion measurements, both are linearly correlated (37). Our control RV perfusion reserves are therefore in general agreement with prior coronary Doppler flow observations.

Hyperemic perfusion measurements and flow resistances in the CCHD patients were comparable to those in controls, suggesting that the patients have a preserved response to pharmacological vasodilatation. In a statistical model, basal perfusion and heart rate, stress systolic blood pressure, and rest and stress arterial oxygen saturations were related to hyperemic perfusion values. It is possible that basal perfusion and basal heart rate may reflect the "set point" of regional tissue oxygen demand and therefore be an indirect determinant of hyperemic perfusion. Also, it is reasonable to consider that stress systolic blood pressure may reflect afterload, a determinant of myocardial oxygen demand, and be related to hyperemic perfusion.

It is intriguing that both rest and stress arterial oxygen saturation were related to hyperemic perfusion. Jagger and colleagues (24) have suggested that the release of ATP from red blood cells in the microcirculation is related to the oxygenation state of hemoglobin. Local release of ATP might provide an additional stimulus for vasodilatation and microcirculatory remodeling beyond that induced by shear stress-mediated changes in flow.

Although our study was not designed to elucidate why CCHD patients have preserved hyperemic perfusion, we believe that this may reflect remodeling of the coronary microcirculation. We did not identify any differences in the PET-derived indexes of coronary vascular resistance between the CCHD patients and controls. The PET measurements reflect the integrated total resistance to blood flow, and an increase in the rheologic component of resistance attending the erythrocytosis associated with CCHD must be compensated for by a decrease in another resistance component if total resistance is to remain unchanged. Several clinical observations suggest that structural remodeling of the resistance vessels is one mechanism that could compensate for the increased viscosity in erythrocytotic CCHD patients. Normal individuals who live at high altitudes and who are chronically hypoxemic are also erythrocytotic. On postmortem examination of the coronary arterial tree, these individuals have an increase in the number of secondary arterial branches leaving the main coronary arteries and an increase in the number of peripheral ramifications compared with those who dwell at sea level (2). Similar microvascular changes might therefore be evoked in hypoxic, erythrocytotic CCHD patients. In our CCHD patients, the observation that basal oxygen delivery to the myocardium is preserved (or even enhanced) relative to the rate pressure product as an indirect measure of cardiac work supports the concept of compensatory microvascular remodeling in these individuals. In addition, initial studies in necropsy specimens indicate that measured arteriolar diameters in Eisenmenger's syndrome patients are 27% larger in diameter than in normal subjects (J. K. Perloff, unpublished observations). Further histopathological studies in CCHD patients are currently underway to examine this possibility.

Hyperemic measurements were not directly related to hematocrits or wall thicknesses. This is expected, because blood viscosity reflects not only red blood cell mass (hematocrit) but also plasma viscosity, plasma protein morphology and concentration, aggregation. and dispersion of cellular elements, and red blood cell morphology and deformability (59). It also is not surprising that perfusion reserves and hyperemic perfusion measurements were unrelated to wall thickness. Because the ventricles in the CCHD patients function against systemic vascular resistances from birth, the increase in mass due to early myocyte replication is accompanied by capillary angiogenesis (49), which serves to help sustain normal capillary density.

Study limitations. Mean hyperemic perfusion values did not differ statistically between the CCHD patients and the normal volunteers. With the use of the 95% confidence limits of 0.33 $ml \cdot min^{-1} \cdot g^{-1}$ for septal and LV free wall PET perfusion measurements, the present study would detect a difference in group means of 0.47 $ml \cdot min^{-1} \cdot g^{-1}$ or greater with 90% power. Similarly, using the 95% confidence limit of 0.57 $ml \cdot min^{-1} \cdot g^{-1}$ for the RV measurements, the present study would detect a difference in the means of the group values of 0.80 $ml \cdot min^{-1} \cdot g^{-1}$ with 90% power. Thus actual but smaller differences in the group means would not have been considered statistically significant. By way of comparison, mean differences of 0.95 $ml \cdot min^{-1} \cdot g^{-1}$ in hyperemic perfusion measurements have been observed between normals and borderline hypertensive patients (33). Even larger mean differences have been identified between normals and those with hyperlipidemia [1.00 $ml \cdot min^{-1} \cdot g^{-1}$ (43)], dilated cardiomyopathy [1.14 $ml \cdot min^{-1} \cdot g^{-1}$ (58)], myocardial hypertrophy [1.36 $ml \cdot min^{-1} \cdot g^{-1}$ (9)], and chronic systemic hypertension [1.39 $ml \cdot min^{-1} \cdot g^{-1}$ (18)].

Because the spatial resolution of the PET tomograph approximates ventricular wall thickness, it was not possible to determine transmural perfusion gradients. In a canine model, cyanotic dogs had lower subendocardial to subepicardial LV blood flow ratios in the basal state and during pharmacological stress (45). Subendocardial perfusion might have therefore differed between the groups and remained undetected.

Measuring RV blood flows in normal controls is challenging. The RV free wall is thin, so that recovered counts are disproportionately smaller than in the left ventricle or septum, and image noise increases. In addition, spillover of vascular activity increases as chamber size decreases. Despite partial volume corrections, small-count fluctuations were likely propagated to the perfusion measurements, contributing to the scatter in our control values. Moreover, the reproducibility of the PET RV perfusion measurements has yet to be determined. In the CCHD patients with thickened RV free walls and chamber dilatation, count fluctuations would be less important, so that the accuracy of the RV determinations should approach those of the LV measurements.

Clinical implications. Patients with CCHD are frequently limited in their ability to exercise (19). Although the factors limiting exercise capacity in CCHD patients remain the object of ongoing clinical investigations, our study indicates that hyperemic myocardial perfusion in these individuals is comparable to that of healthy volunteers. As such, the present investigation does not support the concept that exercise capacity in CCHD patients is diminished by a limitation in achievable hyperemic myocardial perfusion. This contrasts with prior studies in patients with systemic hypertension and ventricular hypertrophy, for example, in which diminished functional capacity appears related to the impairment in myocardial perfusion reserve (1). Rather, prior clinical studies indicate that an impairment in oxygen uptake and reduced ventilatory efficiency are the predominant factors limiting exercise capacity in CCHD patients (19, 54).

An increase in myocardial mass is common in CCHD. In CCHD patients, this arises in the setting of a gross structural abnormality present from birth that is not genetic in origin. In our CCHD patients, hyperemic perfusion was preserved and comparable to that of controls. This differs significantly from observations made previously in patients with acquired hypertrophy due to hypertensive or valvular heart disease (1, 9, 18, 48), in which basal perfusion measurements were normal and hyperemic myocardial perfusion and perfusion reserves were decreased relative to controls. Our observations regarding hyperemic perfusion in the CCHD patients more closely parallel those made in those with the hypertrophy of the "athlete's" heart, in which hyperemic perfusion and perfusion reserves are preserved (21, 26). These observations suggest that there may be significant differences in the pathogenesis and pathophysiology of the increase in ventricular mass between CCHD patients and those with acquired forms of ventricular hypertrophy (hypertensive or valvular heart disease). As such, further investigations appear warranted to elucidate the interrelationships among perfusion, myocyte hyperplasia, myocyte hypertrophy, and oxygen supply/demand, and to define the varying responses of the coronary circulation to an impairment in tissue oxygen supply.

In conclusion, although myocardial perfusion reserve is diminished in adult patients with CCHD, this primarily reflects higher perfusion in the basal state. Calculated oxygen delivery to the myocardium in the basal state is preserved and may even exceed that predicted by a routinely used clinical index of cardiac work, the RPP. Despite the hemodynamic burden imposed by compensatory erythrocytosis, CCHD patients have achievable hyperemic perfusion measurements and coronary vascular resistances during pharmacological stress that are similar to those in normal subjects. These findings suggest a remodeling of the coronary circulation to compensate for the chronic rheologic changes accompanying the systemic arterial hypoxemia in CCHD patients.

GRANTS

The Department of Molecular and Medical Pharmacology is operated for the United States Department of Energy by the University of California under Contract DE-AC03–76-SF00012. This work was supported in part by the Director of the Office of Energy Research, Office of Health and Environmental Research, Washington, D.C., Grant HL-33177 of National Heart, Lung, and Blood Institute and an Investigative Group Award by the Greater Los Angeles Affiliate of the American Heart Association, Los Angeles, California.

REFERENCES

1. **Akinboboye OO, Idris O, Goldsmith R, Berekashvili K, Chou RL, and Bergman SR.** Positron emission tomography, echo-doppler, and exercise studies of functional capacity in hypertensive heart disease. *Am J Hypertens* 15: 907–910, 2002.
2. **Arias-Stella J and Topilsky M.** Anatomy of the coronary circulation at high altitude. In: *High Altitude Physiology: Cardiac and Respiratory Aspects*, edited by Porter R and Knight J. London: Churchill-Livingstone, 1971, p. 149–157.
3. **Berman W, Wood SC, Yabek SM, Dillon T, Fripp RR, and Burstein R.** Systemic oxygen transport in patients with congenital heart disease. *Circulation* 75: 360–368, 1987.
4. **Bellina CR, Parodi O, Camici P, Salvadori PA, Taddei L, Fusani L, Guzzardi R, Klassen GA, L'Abbate A, and Donato L.** Simultaneous in vitro and in vivo validation of nitrogen-13 ammonia for the assessment of regional myocardial blood flow. *J Nucl Med* 31: 1335–1343, 1990.
5. **Bjork L.** Ectasia of the coronary arteries. *Radiology* 87: 33–34, 1966.
6. **Bol A, Melin JA, Vanoverschelde JL, Baudhuin T, Vogelaers D, De Pauw M, Michel C, Luxen A, Labar D, Cogneau M, Robert A, Heyndrickx GR, and Wijns W.** Direct comparison of [^{13}N]ammonia and [^{15}O]water estimates of perfusion with quantification of regional myocardial blood flow by microspheres. *Circulation* 87: 512–525, 1993.
7. **Bongrazio M, Baumann C, Zakrzewicz A, Pries AR, and Gaehtgens P.** Evidence for modulation of genes involved in vascular adaptation by prolonged exposure of endothelial cells to shear stress. *Cardiovasc Res* 47: 384–393, 2000.
8. **Brunken RC, Huang SC, Czernin J, Purcell-Tornai S, and Schelbert HR.** Quantification of right ventricular blood flows with dynamic N-13 ammonia PET imaging (Abstract). *J Nucl Med* 35: 155P, 1994.
9. **Camici P, Chiriatti G, Lorenzoni R, Bellina RC, Gistri R, Italiani G, Parodi O, Salvadori PA, Nista N, Papi L, and L'Abbate A.** Coronary vasodilatation is impaired in both hypertrophied and nonhypertrophied myocardium of patients with hypertrophic cardiomyopathy: a study with nitrogen-13 ammonia and positron emission tomography. *J Am Coll Cardiol* 17: 879–886, 1991.
10. **Child JS.** Transthoracic and transesophageal echocardiographic imaging. In: *Congenital Heart Disease in Adults*, by Perloff JK and Child JS. Philadelphia, PA: Saunders, 1998, p. 91–128.
11. **Chugh R, Perloff JK, Fishbein M, and Child JS.** Extramural coronary arteries in adults with cyanotic congenital heart disease. *Am J Cardiol* 94: 1355–1357, 2004.
12. **Czernin J, Müller P, Chan S, Brunken R, Porenta G, Krivokapich J, Chen K, Chan A, Phelps M, and Schelbert H.** Influence of age and hemodynamics on myocardial blood flow and flow reserve. *Circulation* 88: 62–69, 1993.
13. **DeGrado TR, Hanson MW, Turkington TG, Delong DM, Brezinski DA, Vallee JP, Hedlund LW, Zhang J, Cobb F, Sullivan MJ, and Coleman RE.** Estimation of myocardial blood flow for longitudinal studies with ^{13}N-labeled ammonia and positron emission tomography. *J Nucl Cardiol* 3: 494–507, 1996.
14. **De Wit C, Schafer C, von Bismarck P, Bolz SS, and Pohl U.** Elevation of plasma viscosity induces sustained NO-mediated dilation in the hamster cremaster microcirculation in vivo. *Pflügers Arch* 434: 354–361, 1997.
15. **Di Carli M, Czernin J, Hoh CK, Gerbaudo V, Brunken R, Huang S, Phelps M, and Schelbert H.** Relation among stenosis severity, myocardial blood flow, and flow reserve in patients with coronary artery disease. *Circulation* 91: 1944–1951, 1995.
16. **Gambhir S.** *Quantitation of Physical Factors Affecting the Tracer Kinetic Modeling of Cardiac Positron Emission Tomographic Data* (PhD thesis) (Biomathematics), Los Angeles, CA: Univ. of California, 1990, p. 166.
17. **Giddings S and Stockman J.** Erythropoetin in cyanotic heart disease. *Am Heart J* 116: 128–132, 1988.
18. **Gimelli A, Schneider-Eicke J, Neglia D, Sambuceti G, Giorgetti A, Bigalli G, Parodi G, Pedrinelli R, and Parodi O.** Homogeneously reduced vs. regionally impaired myocardial blood flow in hypertensive patients: two different patterns of myocardial perfusion associated with degree of hypertrophy. *J Am Coll Cardiol* 31: 366–373, 1998.
19. **Glaser S, Opitz CF, Bauer U, Wensel R, Ewert R, Lange PE, and Kleber FX.** Assessment of symptoms and exercise capacity in cyanotic patients with congenital heart disease. *Chest* 125: 368–376, 2004.
20. **Gu JW and Adair TH.** Hypoxia-induced expression of VEGF is reversible in myocardial vascular smooth muscle cells. *Am J Physiol Heart Circ Physiol* 273: H628–H633, 1997.

21. **Hildick-Smith DJR, Johnson PH, Wisbey CR, Winter EM, and Shapiro LM.** Coronary flow reserve is supranormal in endurance athletes: an adenosine transthoracic echocardiographic study. *Heart* 84: 383–389, 2000.
22. **Hutton RD.** The effect of iron deficiency on whole blood viscosity in polycythaemic patients. *Br J Haematol* 43: 191–199, 1979.
23. **Iida J, Rhodes C, Araujo L, Yamamoto Y, de Silva R, Maseri A, and Jones T.** Noninvasive quantification of regional myocardial metabolic rate for oxygen by use of $^{15}O_2$ inhalation and positron emission tomography. *Circulation* 94: 792–807, 1996.
24. **Jagger JE, Bateman RM, Ellsworth ML, and Ellis CG.** Role of erythrocyte in regulating local O_2 delivery mediated by hemoglobin oxygenation. *Am J Physiol Heart Circ Physiol* 280: H2833–H2839, 2001.
25. **Jelkmann W.** Erythropoietin: structure, control of production, and function. *Physiol Rev* 72: 449–489, 1992.
26. **Kalliokoski KK, Nuutila P, Laine H, Luotolahti M, Janatuinen T, Raitakari OT, Takala TO, and Knuuti J.** Myocardial perfusion and perfusion reserve in endurance-trained men. *Med Sci Sports Exerc* 34: 948–953, 2002.
27. **Kershenovich S, Modiano M, and Ewy GA.** Markedly decreased coronary blood flow in secondary polycythemia. *Am Heart J* 123: 521–523, 1992.
28. **King RB, Bassingthwaighte JB, Hales JRS, and Rowell LB.** Stability of heterogeneity of myocardial blood flow in normal awake baboons. *Circ Res* 57: 285–295, 1985.
29. **Koller A, Sun D, and Kaley G.** Role of shear stress and endothelial prostaglandins in flow-and viscosity-induced dilatation of arterioles in vivo. *Circ Res* 72: 1276–1284, 1993.
30. **Kontras SB, Bodenbender JG, Craenen J, and Hosier DM.** Hyperviscosity in congenital heart disease. *J Pediatr* 76: 214–220, 1970.
31. **Krivokapich J, Smith GT, Huang SC, Hoffman EJ, Ratib O, Phelps ME, and Schelbert HR.** ^{13}N ammonia myocardial imaging at rest and with exercise in normal volunteers. Quantification of absolute myocardial perfusion with dynamic positron emission tomography. *Circulation* 80: 1328–1337, 1989.
32. **Kuhle WG, Porenta G, Huang SC, Buxton D, Gambhir S, Hansen H, Phelps M, and Schelbert H.** Quantification of regional myocardial blood flow using ^{13}N-ammonia and reoriented dynamic positron emission tomographic imaging. *Circulation* 86: 1004–1017, 1992.
33. **Laine H, Raitakari OT, Niinikoski H, Pitkanen OP, Iida H, Viikari J, Nuutila P, and Knuuti J.** Early impairment of coronary flow reserve in young men with borderline hypertension. *J Am Coll Cardiol* 32: 147–153, 1998.
34. **Linderkamp O, Klose HJ, Betke K, Brodherr-Heberlein S, Buhlmeyer K, Kelson S, and Sengespeik C.** Increased blood viscosity in patients with cyanotic congenital heart disease and iron deficiency. *J Pediatr* 95: 567–569, 1979.
35. **Marti HH and Risau W.** Systemic hypoxia changes the organ-specific distribution of vascular endothelial growth factor and its receptors. *Proc Natl Acad Sci USA* 95: 15809–15814, 1998.
36. **McGinn AL, White CW, and Wilson RF.** Interstudy variability of coronary flow reserve. Influence of heart rate, arterial pressure, and ventricular preload. *Circulation* 81: 1319–1330, 1990.
37. **Miller DD, Donohue TJ, Wolford TL, Kern M, and Bergmann S.** Assessment of blood flow distal to coronary artery stenoses. Correlations between myocardial positron emission tomography and poststenotic intracoronary Doppler flow reserve. *Circulation* 94: 2447–2454, 1996.
38. **Muzik O, Beanlands RSB, Hutchins G, Mangner TJ, Nguyen N, and Schwaiger M.** Validation of nitrogen-13-ammonia tracer kinetic model for quantification of myocardial blood flow using PET. *J Nucl Med* 34: 83–91, 1993.
39. **Nagamachi S, Czernin J, Kim AS, Sun KT, Bottcher M, Phelps ME, and Schelbert HR.** Reproducibility of measurements of regional resting, and hyperemic myocardial blood flow assessed with PET. *J Nucl Med* 37: 1626–1631, 1996.
40. **Niwa K, Perloff JK, Bhuta S, Laks H, Drinkwater DC, Child JS, and Miner PD.** Structural abnormalities of great arterial walls in congenital heart disease. Light and electron microscopic analyses. *Circulation* 103: 393–400, 2001.
41. **Perloff JK Urschell CW, Roberts WC, and Caulfield WH.** Aneurysmal dilatation of the coronary arteries in cyanotic congenital cardiac disease. *Am J Med* 45: 802–810, 1968.
42. **Perloff JK.** Systemic complications of cyanosis in adults with congenital heart disease. *Cardiol Clin* 11: 689–699, 1993.
43. **Pitkanen OP, Nuutila P, Raitakari OT, Porkka K, Iida H, Nuotio I, Ronnemaa T, Viikari J, Taskinen MR, Ehnholm C, and Knuuti J.** Coronary flow reserve in young men with familial combined hyperlipidemia. *Circulation* 99: 1678–1684, 1999.
44. **Porenta G, Kuhle W, Czernin J, Ratib O, Brunken RC, Phelps ME, and Schelbert HR.** Semiquantitative assessment of myocardial blood flow and viability using polar map displays of cardiac PET images. *J Nucl Med* 33: 1628–1636, 1992.
45. **Pridjian AK, Bove EL, and Lupinetti FM.** The effects of cyanosis on myocardial blood flow, oxygen utilization, and lactate production in dogs. *J Thoracic CV Surg* 109: 849–853, 1995.
46. **Pries AR, Secomb TW, Gessner T, Sperandio MB, Gross JF, and Gaehtgens P.** Resistance to blood flow in microvessels in vivo. *Circ Res* 75: 904–915, 1994.
47. **Pries AR, Reglin B, and Secomb TW.** Structural response of microcirculatory networks to changes in demand: information transfer by shear stress. *Am J Physiol Heart Circ Physiol* 284: H2204–H2212, 2003.
48. **Rajappan K, Rimoldi OE, Camici P, Bellenger N, Pennell D, and Sheridan DJ.** Functional changes in coronary microcirculation after valve replacement in patients with aortic stenosis. *Circulation* 107: 3170–3175, 2003.
49. **Rakusan K, Flanagan MF, Geva T, Southern J, and Van Praagh R.** Morphometry of human capillaries during normal growth and the effect of age in left ventricular pressure-overload hypertrophy. *Circulation* 86: 38–46, 1992.
50. **Ranjan V, Xiao Z, and Diamond SL.** Constitutive NOS expression in cultured endothelial cells is elevated by fluid sheer stress. *Am J Physiol Heart Circ Physiol* 269: H550–H555, 1995.
51. **Rudolph W.** Myocardial metabolism in cyanotic congenital heart disease. *Cardiology* 56: 209–215, 1971.
52. **Sawada S, Muzik O, Beanlands RSB, Wolfe E, Hutchins GD, and Schwaiger M.** Interobserver and interstudy variability of myocardial blood flow and flow-reserve measurements with nitrogen-13 ammonia labeled positron emission tomography. *J Nucl Cardiol* 2: 413–422, 1995.
53. **Scheuer J, Shaver JA, Kroetz FW, and Leonard L.** Myocardial metabolism in cyanotic congenital heart disease. *Cardiology* 55: 193–210, 1970.
54. **Sietsema KE, Cooper DM, Perloff JK, Rosove MH, Child JS, Canobbio MM, Whipp BJ, and Wasserman K.** Dynamics of oxygen uptake during exercise in adults with cyanotic congenital heart disease. *Circulation* 73: 1137–1144, 1986.
55. **Snider RA and Serwer GA.** Methods for obtaining quantitative information from the echocardiographic examination. In: *Echocardiography in Pediatric Heart Disease,* edited by Snider RA and Serwer G. A. Chicago, IL: Year Book Medical, 1990, p. 78–133.
56. **Tulis DA, Unthank JL, and Prewitt RL.** Flow-induced arterial remodeling in rat mesenteric vasculature. *Am J Physiol Heart Circ Physiol* 274: H874–H882, 1998.
57. **Tuttle JL, Nachreiner RD, Bhuller AS, Condict KW, Connors BA, Herring BP, Dalsing MC, and Unthank JL.** Shear level influences resistance artery remodeling: wall dimensions, cell density, and eNOS expression. *Am J Physiol Heart Circ Physiol* 273: H628–H633, 1997.
58. **Van den Heuvel AFM, van Veldhuisen DJ, van der Wall EE, Blanksma PK, Siebelink HMJ, Vaalburg WM, van Gilst WH, and Crijns HJGM.** Regional myocardial blood flow reserve impairment and metabolic changes suggesting myocardial ischemia in patients with idiopathic dilated cardiomyopathy. *J Am Coll Cardiol* 35: 19–28, 1999.
59. **Wells R.** Syndromes of hyperviscosity. *N Engl J Med* 283: 183–186, 1970.
60. **Wilson RF, Laughlin DE, Ackell PH, Chilian WM, Holida MD, Hartley CJ, Armstrong ML, Marcus ML, and White CW.** Transluminal, subselective measurement of coronary artery blood flow velocity and vasodilator reserve in man. *Circulation* 72: 82–92, 1985.
61. **Yeager SB and Freed MD.** Myocardial infarction as a manifestation of polycythemia in cyanotic heart disease. *Am J Cardiol* 53: 952–953, 1984.